Application of Cosserat Continuum Model for Analysis of Excavations in Layered Rock Masses

H. Bidhendi
Hatch Mott MacDonald, Mississauga, Ontario, Canada
A. Riahi & J.H. Curran
Rocscience Inc., Toronto, Ontario, Canada

ABSTRACT
This paper focuses on the analysis of tunnelling problems in layered rocks using the Cosserat continuum approach. In the Cosserat continuum method, the interfaces between rock layers need not be explicitly modelled. Instead, the internal characteristic length, i.e., the layer thickness and the interaction condition between the layers are incorporated in the governing equations. Two tunnelling problems, an extruded tunnel excavated in layered rock and a circular tunnel with out-of-plane layers which requires a full 3D analysis, are solved using the Cosserat continuum finite element method. Results of the Cosserat approach are verified against alternative approaches. The paper demonstrates that Cosserat continuum approach can provide a mechanically-based yet efficient solution for the analysis of engineering scale discrete problems.

RÉSUMÉ
Cet article porte sur l'analyse des problèmes associés aux tunnels aménagés dans des roches stratifiées en utilisant l'approche du continuum de Cosserat. Dans la méthode du continuum de Cosserat, les interfaces entre les couches de roche n'ont pas besoin d'être modélisées de façon explicite. Au lieu de cela, la longueur interne caractéristique, c'est-à-dire l'épaisseur de la couche et les conditions d'interaction entre les couches est incorporée dans les équations constitutives. Deux problèmes sont résolus à l'aide de la méthode des éléments finis et de l'approche du continuum de Cosserat, soit un tunnel extrudé et creusé dans une roche stratifiée et un tunnel circulaire ayant des couches obliques par rapport au tunnel et qui exigent une analyse complète en 3D. Les résultats obtenus par l'approche du continuum de Cosserat sont comparés à ceux obtenus par des approches alternatives. Cet article montre comment l'approche du continuum de Cosserat peut apporter une solution efficace basée sur la mécanique des matériaux pour l'analyse des problèmes discrets de grande échelle dans laquelle les effets d'échelle sont importants.

1 INTRODUCTION

Heterogeneities in geomaterials are prevalent in various forms such as fractures, joints, bedding planes, voids, and material boundaries. Such features pose great challenges to the understanding and predicting the complex range of behaviour of geomaterials. Also, they make numerical simulation of this class of materials challenging.

The presence of joints greatly affects the stress distribution and deformation of rock engineering problems, and gives rise to various failure mechanisms due to scale effects. For example, in layered rocks, the impact of joints on tunnelling becomes particularly significant when layer thickness is comparable to the dimensions of the excavation.

The mechanisms arising due to rock microstructure (layers) depend on the strength and mechanical condition between the layers (friction, sliding, and interface stiffness), joint orientation, and spacing. Effects of joints on the response of rock masses have long been represented using smeared (homogenous) concepts. For example, many strength criteria have been proposed that reflect the interconnection between presence of discontinuous surfaces with strength deterioration and anisotropic behaviour. These constitutive models tend to reflect large-scale effects of joint density and the condition of joint surfaces defined by their material parameters. Clearly, such approaches are incapable of predicting different mechanisms associated with internal length scales.

Fortunately, rock mechanics has reached a point where it is well accepted that scale effects are an important aspect of jointed rock mass behaviour. In other words, jointed rock masses cannot be treated as standard continua. As a result, numerical methods that simulate the discontinuities seem to be essential.

Three approaches are commonly used to model the discontinuous behaviour of jointed rock masses. These are:

1. Discrete element techniques, and their combined discrete-continuum derivatives,
2. Combined continuum-interface methods, which are continuum methods with special joint/interface elements that model discontinuous displacement behaviour, and
3. Cosserat continuum methods.

Choosing between continuum and discontinuum methods for modelling jointed rock masses has been the subject of much debate in recent years. Due to their discrete nature, discontinuous models seem to be the natural choice for analysis. Discrete element techniques are based on a fully dynamic formulation and require algorithms for updating contacting pairs and calculating contact forces. These aspects considerably affect the solution time. Also, explicit definition of discontinuous interfaces complicates creating model geometry.

Continuum-based methods such as the Finite Element Method (FEM) and the Finite Difference Method (FDM) are based on solid theoretical foundations and enjoy a long history of development. Nevertheless, they suffer from some inherent deficiencies due to the very nature of a continuous description of media. Joint elements are devised specially to reflect the discontinuity in displacement at the interfaces of two layers. Combined continuum-interface techniques have been shown to be capable of capturing some fundamental effects of discontinuities on the behaviour of discrete media including anisotropy, strength behaviour, and scale effects. Due to the assumed kinematics of a joint element and the fixed connectivity between its nodes, the most appropriate use of a joint element is in the modeling of problems where pairing between two contacting objects does not change (Riahi et al. 2010). Compared to the discrete element techniques, the combined continuum-joint element approach provides a much more efficient numerical tool in the solution range where displacements of discrete blocks is insignificant. However, they also suffer from deficiencies shared by the discrete element techniques in defining complex input geometries. The problems associated with model geometry can become insurmountable in the three-dimensional modelling of jointed rock masses with intersecting sets of joints when the resulting blocks need to be further discretized into a mesh or grid.

In order to harness the advantages of fully continuum methods we need to resort to advanced continuum theories such as micropolar continuum theories. These theories enhance the mechanics of the classical continuum by introducing intrinsic length scales into the governing equations. The Cosserat continuum is considered as a subclass of generalized continua. It assumes additional rotational degrees of freedom for each material point. As a result, in addition to gradient of displacement (strains), gradients of rotations (curvatures) also appear in the governing equations (Eringen, 1999; Eringen, 2002; Forest, 2005).

Recent advances in the finite element formulation of the Cosserat continuum framework for analysis of layered rocks (Mühlhaus (1993; 1995), Adhikary et al. (1997; 1999; 2007), Riahi et al. (2008; 2009)) are testament to the capabilities of enhanced continuum methods in modelling complex responses of geomaterials. These works show that the Cosserat continuum method is capable of predicting some fundamental behaviour arising from the presence of discontinuous surfaces including anisotropy, complex strength response due to failure of joints or intact rock, and mechanisms controlled by internal lengths such as bending and buckling of rock layers.

2 COSSERAT CONTINUUM

Perhaps the most natural way of enhancing the classical continuum representation is to consider rotational degrees of freedom for each material point in addition to the translational degrees of freedom. The first rigorous formulation of the idea of a material body enhanced with independent rotational degrees of freedom dates back to the seminal work of the Cosserat brothers (Cosserat and Cosserat, 1909).

The basic kinematic variables of Cosserat theory are the displacements, the first-order displacement gradients (normal and shear stains), the microstructural rotations, and the rotation gradients (curvatures).

In Cosserat theory, in addition to the stress-strain work conjugate pair, micromoment-curvature is another kinetic-kinematic work conjugate pair which is introduced into the governing equations. A direct consequence of introducing the micromoment-curvature work conjugate pair is to relax the stress tensor symmetry. The resulting differences in the shear components of the stress tensor are then equilibrated by micromoments.

The appealing aspect of Cosserat continuum theory is that the additional constitutive relations between micromoments and curvatures incorporate the effects of material microstructure. As a result, Cosserat continuum theory can capture scale effects and provides a mechanically enhanced yet homogeneous description of materials with microstructure. For example, in the case of layered media, the bending stiffness of individual layers is incorporated into the constitutive equations, distinguishing the model from conventional treatments.

3 GOVERNING EQUATIONS, MICROPOLAR STRESS AND MICROPOLAR COUPLE STRESS

Cosserat theory assumes that micromoments exist at each point of the continuum. In Cosserat theory, equilibrium of forces and moments are expressed in the following form[1] (Truesdell and Toupin 1960):

$$\sigma_{ij,i} + b_j = 0, \qquad [1]$$

$$m_k + \mu_{kj,j} + e_{kij}\sigma_{ij} = 0, \qquad [2]$$

where **b** is the body force, **m** is the body couple moment, and **σ** and **μ** are the Cosserat stress and Cosserat couple stress, or moment stress, respectively. The stress tensor **σ** is analogous to the Cauchy stress of the classical continuum. Also, the stress vector or stress traction and

[1] Note: Within this text bold notation represents vector or tensor quantities; single sub-index refers to components of vectors and double sub-indices denote components of second rank tensors or matrices.

the couple stress vector or moment traction are defined by

$$\mathbf{t}_{\sigma}=\boldsymbol{\sigma}\cdot\mathbf{n} \text{ and } \mathbf{t}_{m}=\boldsymbol{\mu}\cdot\mathbf{n}, \qquad [3]$$

where **n** is the normal to the surface.

Fig. 1 represents the stress and couple stress measures for a 3D representative volume. The first subscript of the stress tensor refers to the direction of the surface normal of the surface on which the stress acts. The second subscript of the stress refers to the direction that the stress acts. The first subscript of the couple stress (or moment stress) refers to the axis about which it causes rotation, while the second subscript denotes the surface on which the moment stress acts. The notation adopted for stress tensor components is similar to the standard notation used in classical continuum theory; however, it is different from the notation of some of the previous works on Cosserat theory referred in this paper (Mühlhaus, 1993; Adhikary and Dyskin, 2007). The notation adopted for couple stress components is compatible with most literature on Cosserat theory; however, it differs from the ordinary notation used in plate theory, where the moment subscript refers to the stress components by which the moments are produced (i.g., $M_x=\int_{-h/2}^{+h/2}\sigma_{xx}zd_z$ (Szilard 2004).

In the absence of body moment and when couple stress terms are self-equilibrated, the condition of symmetry of the Cauchy stress and its work conjugate strain measure is retrieved, and the Cosserat continuum reduces to the classical continuum.

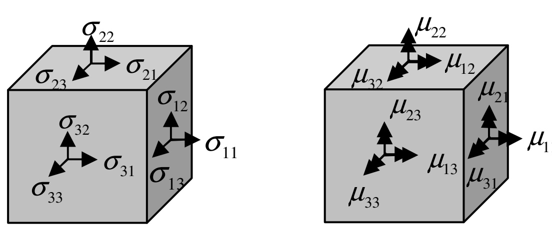

Figure 1. 3D representation of stress and couple stress measures.

3.1 Cosserat Rotations

Compared to a classical continuum, an enhanced or Cosserat continuum is obtained by adding rotational degrees of freedom to each point of the continuum. Cosserat rotation is defined as the independent rotation of a rigid triad attached to each material point which rotates independently with respect to the material triad. In a 2D framework, the Cosserat rotation has one component about the out-of-plane direction. In a three-dimensional framework, however, the Cosserat rotation has three independent components about axes of the orthogonal coordinate system. The Cosserat rotation is represented in the matrix form by

$$\mathbf{R}^{\mathbf{c}}=\begin{pmatrix}1 & -\theta_3 & \theta_2\\ \theta_3 & 1 & -\theta_1\\ -\theta_2 & \theta_1 & 1\end{pmatrix}. \qquad [4]$$

For further details on the mathematical description of the Cosserat continuum in a general (large deformation) framework, refer to (Steinmann 1994).

3.2 Cosserat Strain

Using the principle of virtual work, the Cosserat strain measure $\boldsymbol{\gamma}$, which is the work conjugate to $\boldsymbol{\sigma}$, is defined in the following form:

$$\gamma_{ij}=u_{j,i}-\varepsilon_{ijk}\theta_k \quad , \qquad [5]$$

where ε_{ijk} is the permutation symbol.

3.3 Cosserat Curvature

In a continuum with microstructure, in addition to the rotation of the rigid triad with respect to the material (reference) triad, which is defined as the Cosserat rotation, the variation in the rotations of adjacent triads is a second measure of deformation referred to as curvature. The expression for the second-order curvature tensor in a three-dimensional framework becomes

$$\boldsymbol{\kappa}=\begin{pmatrix}\kappa_{11} & \kappa_{12} & \kappa_{13}\\ \kappa_{21} & \kappa_{22} & \kappa_{23}\\ \kappa_{31} & \kappa_{32} & \kappa_{33}\end{pmatrix}=\begin{pmatrix}-\theta_{1,1} & -\theta_{1,2} & -\theta_{1,3}\\ -\theta_{2,1} & -\theta_{2,2} & -\theta_{2,3}\\ -\theta_{3,1} & -\theta_{3,2} & -\theta_{3,3}\end{pmatrix} \quad \text{or} \qquad [6]$$

$$\kappa_{ij}=-\theta^{c}_{i,j}\ .$$

4 FINITE ELEMENT FORMULATION

4.1 Nodal and internal variables

In the FEM formulation of a Cosserat continuum, each node *N* is associated with three displacement and three rotational degrees of freedom. The vector of nodal degrees of freedom is defined as

$$\bar{\mathbf{U}}=\begin{bmatrix}\bar{\mathbf{u}} & \bar{\boldsymbol{\theta}}\end{bmatrix}=[\bar{u}_1 \quad \bar{u}_2 \quad \bar{u}_3 \quad \bar{\theta}_1 \quad \bar{\theta}_2 \quad \bar{\theta}_3]\ . \qquad [7]$$

Using a notation similar to Voigt notation, the second-order strain and curvature tensors can be expressed in the following vector form:

$$\boldsymbol{\gamma}=[\gamma_{11} \ \ \gamma_{22} \ \ \gamma_{33} \ \ \gamma_{23} \ \ \gamma_{32} \ \ \gamma_{13} \ \ \gamma_{31} \ \ \gamma_{12} \ \ \gamma_{21}]\,, \qquad [8]$$
$$\boldsymbol{\kappa}=\left[\kappa_{11} \ \ \kappa_{22} \ \ \kappa_{33} \ \ \kappa_{23} \ \ \kappa_{32} \ \ \kappa_{13} \ \ \kappa_{31} \ \ \kappa_{12} \ \ \kappa_{21}\right].$$

Finally, using FEM discretization technique with the interpolation function, ϕ, the strain and curvature field can be interpolated with respect nodal values of $\overline{\mathbf{u}}_{\mathrm{N}}$ and $\overline{\boldsymbol{\theta}}_{\mathrm{N}}$ through

$$\begin{bmatrix}\boldsymbol{\gamma}\\ \boldsymbol{\kappa}\end{bmatrix}=\mathbf{B}_{\mathrm{N}}\begin{bmatrix}\overline{\mathbf{u}}_{\mathbf{N}}\\ \overline{\boldsymbol{\theta}}_{\mathbf{N}}\end{bmatrix}. \qquad [9]$$

The operator $\mathbf{B}_{\mathrm{N}}$ has a block structure and is expressed in the following form:

$$\mathbf{B}_{\mathrm{N}}=\begin{pmatrix}\mathbf{B}_{\mathrm{N1}} & \mathbf{B}_{\mathrm{N2}}\\ [\mathbf{0}]_{9\times 3} & \mathbf{B}_{\mathrm{N3}}\end{pmatrix}, \qquad [10]$$

with

$$\mathbf{B}_{N1}=\begin{pmatrix}\phi_{N,1} & 0 & 0 & 0 & 0 & 0 & \phi_{N,3} & 0 & \phi_{N,2}\\ 0 & \phi_{N,2} & 0 & 0 & \phi_{N,3} & 0 & 0 & \phi_{N,1} & 0\\ 0 & 0 & \phi_{N,3} & \phi_{N,2} & 0 & \phi_{N,1} & 0 & 0 & 0\end{pmatrix}^{T}, \qquad [11]$$

$$\mathbf{B}_{N2}=\begin{pmatrix}0 & 0 & 0 & -\phi_{N} & \phi_{N} & 0 & 0 & 0 & 0\\ 0 & 0 & 0 & 0 & 0 & \phi_{N} & -\phi_{N} & 0 & 0\\ 0 & 0 & 0 & 0 & 0 & 0 & 0 & -\phi_{N} & \phi_{N}\end{pmatrix}^{T},$$

and

$$\mathbf{B}_{N3}=-\begin{pmatrix}\phi_{N,1} & 0 & 0 & 0 & 0 & \phi_{N,3} & 0 & \phi_{N,2} & 0\\ 0 & \phi_{N,2} & 0 & \phi_{N,3} & 0 & 0 & 0 & 0 & \phi_{N,1}\\ 0 & 0 & \phi_{N,3} & 0 & \phi_{N,2} & 0 & \phi_{N,1} & 0 & 0\end{pmatrix}^{T},$$

where ϕ_N is the shape function for the N^{th} node and is used for interpolation of both the displacement field and the rotation field.

4.2 Material stiffness matrix

Similar to the approach adopted in the derivation of the finite element formulation of the classical continuum, the FEM Cosserat formulation can be obtained by applying the principle of virtual work.

The material stiffness matrix is expressed in the following form:

$$\mathbf{K}_{\mathrm{NM}}^{\mathrm{mat}}=\mathbf{B}_{\mathrm{N}}{}^{\mathrm{T}}\mathbf{D}\mathbf{B}_{\mathrm{M}}, \qquad [12]$$

where $\mathbf{B}$ is defined by Equations (10) and (11), and $\mathbf{D}$ is a block diagonal matrix which relates the stress and couple stress measures to their work conjugate measures, strains and curvatures, respectively, through the appropriate constitutive law $\mathbf{D}=[\mathbf{D_1}, \mathbf{D_2}]$.

4.3 Constitutive Equations

Cosserat continuum theory provides an enhanced mathematical description of the mechanics of a deformable body by introducing higher-order kinetic and kinematic variables. The appealing aspect of the Cosserat theory is that these kinetic and kinematic variables can be linked to the physical behaviour of materials with microstructure (particulate, blocky, or layered material) by mechanically-based approaches. The additional Cosserat parameters should be determined based on the mechanical response of a material with a particular microstructure. In the case of a layered material, the bending stiffness of the individual layers plays a significant role in the overall response of the material. Constitutive equations for the particulate (Mühlhaus and Vardoulakis 1987), layered and blocky (Mühlhaus 1993 and 1995) materials in a two-dimensional framework have been widely discussed. The following constitutive relations are proposed for layered materials in a three-dimensional framework (Riahi 2008, and Riahi and Curran 2009),

$$\mathbf{D}_1=\begin{bmatrix}\mathbf{A_n} & [0]_{3\times 6}\\ [0]_{6\times 3} & \mathbf{A_G}\end{bmatrix}, \quad \mathbf{A}_n=\begin{bmatrix}A_{11} & A_{12} & A_{13}\\ A_{21} & A_{22} & A_{23}\\ A_{31} & A_{32} & A_{33}\end{bmatrix}, \qquad [13]$$

$$\mathbf{A}_G=\begin{bmatrix}G_{22} & G_{11} & 0 & 0 & 0 & 0\\ G_{11} & G_{11} & 0 & 0 & 0 & 0\\ 0 & 0 & G_{22} & G_{11} & 0 & 0\\ 0 & 0 & G_{11} & G_{11} & 0 & 0\\ 0 & 0 & 0 & 0 & G_{11} & G_{11}\\ 0 & 0 & 0 & 0 & G_{11} & G_{11}\end{bmatrix},$$

$$\mathbf{D}_2=\begin{bmatrix}\begin{bmatrix}\begin{bmatrix}(1-\nu)B & 0\\ 0 & (1-\nu)B\end{bmatrix}_{2\times 2} & [0]_{2\times 5}\\ [0]_{5\times 2} & [0]_{5\times 5}\end{bmatrix} & [0]_{7\times 2}\\ [0]_{2\times 7} & \begin{bmatrix}B & \nu B\\ \nu B & B\end{bmatrix}\end{bmatrix}, \qquad [14]$$

and

$$A_{11} = A_{22} = \frac{E}{1-\nu^2 - \dfrac{\nu^2\left(1+\nu\right)^2}{(1-\nu^2 + E/hk_n)}}, \quad [15]$$

$$A_{33} = \frac{(1-\nu)E}{(1+\upsilon)(1-2\upsilon) - \dfrac{(1-\upsilon)E}{(E/hk_n)}},$$

$$A_{12} = A_{21} = \frac{\nu E}{\left(1+\nu\right)\left(1-2\nu\right)+\left(1-\nu\right)E/hk_n},$$

$$A_{13} = A_{31} = A_{23} = A_{32} = \frac{E\nu\left(E+hk_n\left(1-\nu\right)\right)}{\left(1-\nu\right)\left(2hk_n\nu^2-\left(1+\nu\right)\left(E+hk_n\right)\right)}$$

$$G_{11} = \frac{Ghk_2}{G+hk_s}, \quad G_{22} = G + G_{11},$$

$$B = \frac{Eh^2}{12(1-\upsilon^2)}\left(\frac{G-G_{11}}{G+G_{11}}\right).$$

In the above relations, E, G and υ correspond to Young's modulus, shear modulus, and Poisson's ratio, respectively, of the intact material comprising the layers. h is the layer thickness, and k_n and k_s are the normal and shear stiffness of the layer interface.

Finally, it should be noted that the above constitutive equations are based on the mechanical considerations of a plate component (Szilard 2004). For a thorough treatment of FEM formulation and constitutive equations refer to Riahi (2008), and Riahi et al. (2009). Here only the constitutive relations are briefly included to facilitate interpretation of results.

5 ANALYSIS OF TUNNELS IN LAYERED ROCK

In this section, the FEM Cosserat model is used to analyse tunnel excavations in layered rock. The results predicted by the FEM Cosserat model are compared to those predicted by other numerical methods using commercially available software packages.

5.1 Analysis of excavation with in-plane layers

This example concerns analysis of an excavation in layered rock. The layers are parallel to the tunnel axis.

The primary purpose of this example is to investigate how layers and the subsequent induced anisotropy affect the elastic and elasto-plastic response of excavations. For various anisotropy orientations (dip angles from 0 (horizontal joints) to 90 deg. (vertical joints)), the elastic and elasto-plastic response of the problem is studied. The results predicted by the FEM Cosserat model are verified against those predicted by Phase^2 . In Phase^2 layers are explicitly modeled using joint elements (Rocscience, 2005).

The geometry, boundary conditions and mesh discretization for the FEM Cosserat solution of this problem are shown in Figure 2. For all four input models with different joint orientations (presented in Figure 3), the FEM mesh used in the Cosserat solution remains unchanged. The top boundary is subjected to a uniform pressure of 100 MPa. All other boundaries are fixed. In the elasto-plastic solution the load was applied in 10 increments. In order to compare the results with those predicted by Phase^2, in the 3D Cosserat model the displacements associated with the out-of-plane direction (u_y) and the Cosserat rotation around the x axis (θ_x) are constrained. As a result, the full 3D model behaves similarly to a 2D plane strain problem, and therefore it is justified to use one element in the out-of-plane direction.

The intact rock is modelled as an isotropic Mohr-Coulomb material with a Young's modulus of 17.8 GPa, Poisson's ratio of 0.25, friction coefficient of 33.5 deg., dilation angle of 16.72 deg., cohesion of 10.28 MPa, and tensile strength of 0.5 MPa. The joints are spaced 2.5 m apart and exhibit a Mohr-Coulomb failure behaviour with a friction coefficient of 30 deg., dilation angle of 30 deg., and cohesion of 0.5 MPa, with no tensile strength.

For each input model, the elastic response is investigated for two cases: i) k_n=20 GPa/m and k_s=200 MPa/m, and ii) k_n/E=1e10 and k_s=200 MPa/m. Also, using the FEM ubiquitous joint model, it is investigated how neglecting the layer thickness would affect the results. The ubiquitous joint model is a limiting case of the Cosserat model in which the elastic and elasto-plastic properties of the material are modified to take into account the orientation and mechanical response of joints; however, joint spacing or bending stiffness of the layers is disregarded (B=0).

Figure 4 shows the displacement contours predicted by the Cosserat model and Phase^2 model.

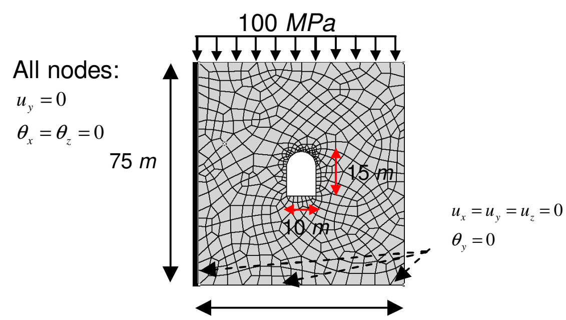

Figure 2. Geometry, mesh discretization, and boundary conditions for the FEM Cosserat solution of a 2D-extruded tunnel excavated in layered rock.

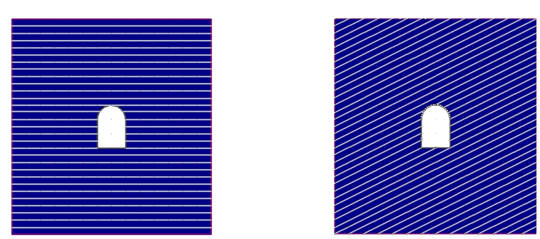

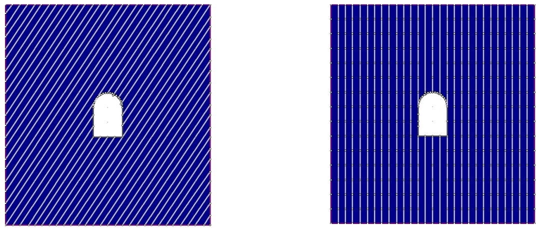

Figure 3. Geometry and joint orientation and spacing for the 2D-extruded tunnel excavated in layered rock.

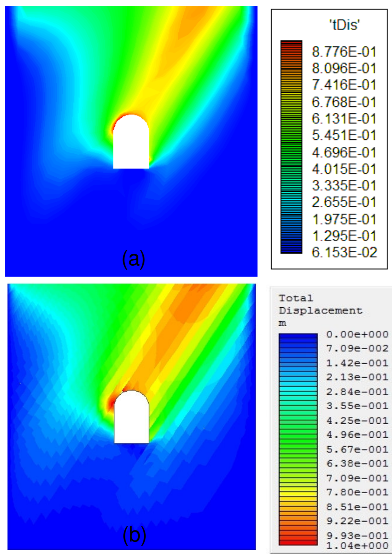

Figure 4. Contours of total elasto-plastic displacement predicted by (a) FEM Cosserat model, and (b) FEM explicit joint model, for joints oriented at 60° with respect to a horizontal plane.

Figure 5 shows the displacements at the centre of the tunnel roof predicted by the Cosserat model, Phase^2 model with explicit representation of the joints, and the ubiquitous joint model. For details on the formulation of Cosserat plasticity refer to Riahi and Curran (2008).

Comparison of the results show that the Cosserat model is capable of predicting both magnitudes and patterns of displacement correctly.

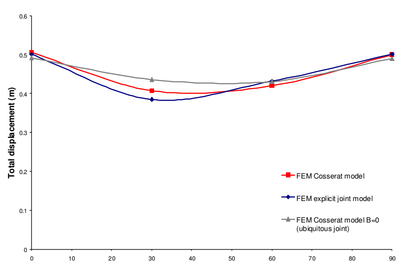

(a)

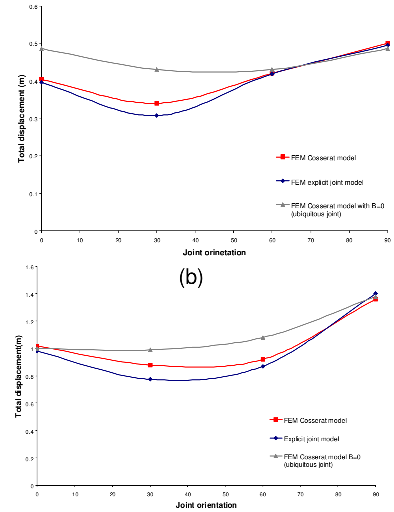

(c)

Figure 5. (a) Total elastic displacement at the center of the tunnel roof for joints with k_n=20000 MPa/m and k_s=200 MPa/m; (b) Total elastic displacement at the center of the tunnel roof for joints with k_n/E =1e10 and k_s=200 MPa/m; (c) Total elasto-plastic displacement at the center of the tunnel roof for joints with k_n=20000 MPa/m and with k_s=200 MPa/m.

5.2 Analysis of excavation with out-of-plane layers

This example investigates the elastic and elasto-plastic response of a circular hole, with a radius of 3m, excavated in a layered rock mass. The layers are dipping at an angle varying from 0 deg. to 90 deg. with respect to the tunnel axis. Figures 6 and 7 show the geometry, boundary conditions, and the joint orientation and spacing for this problem. The length of the extrusion is 60 m and a distributed load with a magnitude of 100 MPa/m is applied over a width of 9 m on the top surface. Due to symmetry, in the FEM Cosserat model, half of the problem is simulated using 2430 brick elements (20-noded). The intact material is an isotropic rock with Young’s modulus of 20 GPa and Poisson’s ratio of 0.3. The intact material and the joints exhibit a Mohr-Coulomb shear failure along with a tension-cut-off. The elasto-plastic material parameters for the intact rock and the joints are presented in Table 1.

The results predicted by the 3D FEM Cosserat model are compared to those predicted by the discrete element technique using 3DEC (Itasca) with deformable blocks.

Figures 8 and 9 show the contours of total displacement predicted by the FEM Cosserat model and 3DEC, for layers dipping at 30 deg. and 60 deg. with respect to the tunnel axis.

Figure 10 shows values of maximum displacement at the tunnel roof for a number of layer orientations. Two different values of layer thickness are considered in this example: h=1.5 m and h=3 m. Also, the error of the solution predicted by the ubiquitous joint model is investigated by reducing bending stiffness of the layers, B, to zero. As previously discussed, the conventional ubiquitous joint model is a limit case of the Cosserat model in which bending stiffness of the layers is disregarded.

Comparison of the results presented in Figures 8-10 shows that the results predicted by the Cosserat model are in good agreement with those predicted by the discrete element approach.

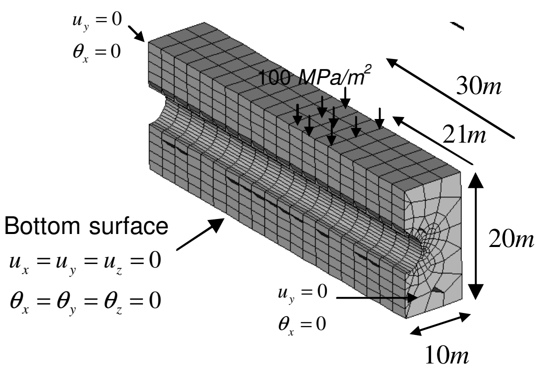

Figure 6. Geometry, boundary conditions, and mesh discretization of the FEM Cosserat model for Example 2; element type: 20-noded brick; number of elements: 2420, number of elements in out-of plane direction: 20, number of FEM nodes:48696, number of DOF in 3D: 11565.

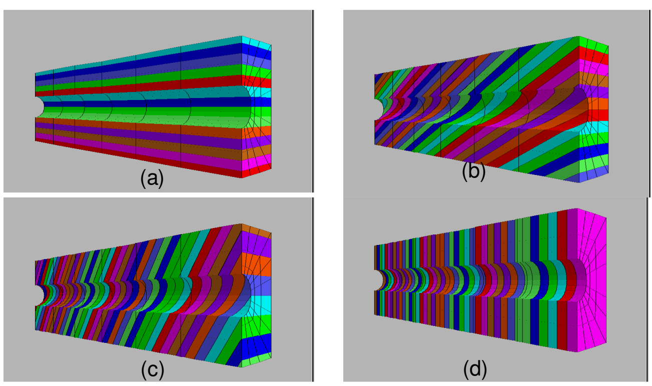

Figure 7. 3DEC model for joints dipping (a) 0°, (b) 30°, (c) 60°, and (d) 90°.

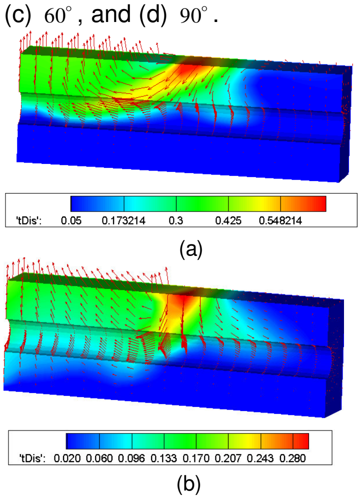

Figure 8. Contours of elasto-plastic displacement for layers dipping at (a) 30° ,(b) 60° predicted by the FEM Cosserat solution joints.

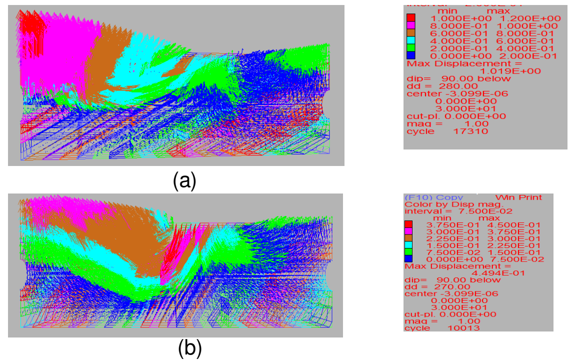

Figure 9. Contours of total elasto-plastic displacement for layers dipping at (a) 30° , (b) 60° predicted by 3DEC.

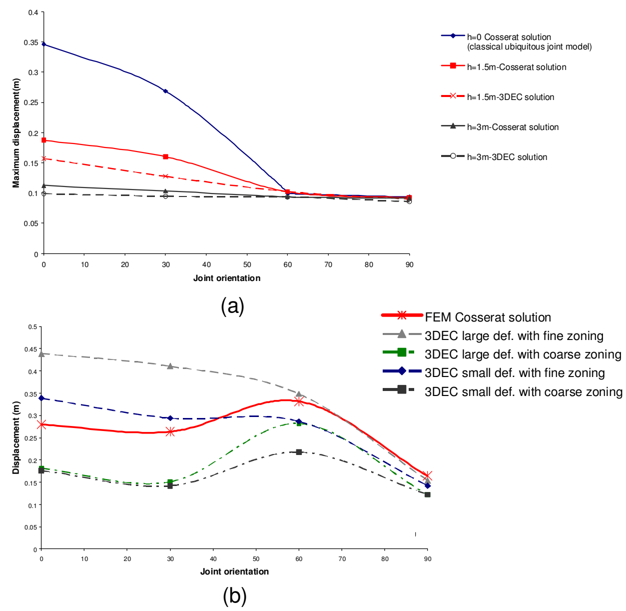

Figure 10. Maximum displacement at the tunnel roof versus joint orientation (a) elastic model (b) elasto-plastic model.

Table 1. Strength properties of the material with out-of plane layers.

Intact rock parameters			
c	φ	φ_{dil}	σ_t
MPa	deg.	deg.	MPa
20	33.5	16.72	1
Joint parameters			
c	φ	φ_{dil}	σ_t
MPa	deg.	deg.	MPa
1	30	0	0.0001

6 CONCLUDING REMARKS

Computational techniques for modelling jointed rock problems have evolved from a continuous notion to a discontinuous one in recent years. As numerical models evolve, they provide better insight into the complex behaviour of geomaterials. They also offer more reliable prediction tools for design engineers.

Rock masses, in general, exhibit a wide range of behaviour associated with different mechanisms. These mechanisms can be in form of slip failure on the joint planes or shear failure of the intact rock, fracture propagation, instability failures such as buckling, and kinematic failures such as detachment of blocks.

Models that intend to capture the whole range of behaviour require adopting a combined discrete-continuum approach or micromechanical approaches such as the synthetic rock mass technique. Clearly, the resources required for such analyses make them impractical for most engineering scale geotechnical problems. A pragmatic solution to rock mechanics problems requires that the critical features and the dominant responses be captured in a timely manner using reasonable computational resources.

There are two aspects that we believe are paramount to the successful application of these techniques in research and practice:

1. Numerical models should account for the characteristic physics and micromechanics of the problem through proper mechanical representation of materials. Such approaches eliminate the need for complicated empirical constitutive models and associated parametric adjustment techniques.
2. Numerical models must be specific purpose. In other words, the paramount aspects of the behaviour and the range of response should guide the development and application of a numerical method.

The first aspect noted above addresses the growing need for more physically-based models. The second is due to the need for solutions that can overcome practical problems associated with defining input geometry, required solution time, and computational resources.

The dimensions of typical excavation problems are such that explicit definition of material microstructures through interface elements or discrete element techniques makes creating the input geometry challenging and requires high computational resources. The complexities become even more restrictive in three-dimensional analyses, stochastical approaches, or determining safety factor through the shear strength reduction approach.

On the other hand, without proper consideration of material microstructure such as inter-layer interaction, and internal lengths, deformation and failure mechanisms cannot be correctly predicted.

This paper shows that the FE-Cosserat model can be regarded as a method that meets both of the aforementioned criteria. The Cosserat continuum approach provides a smeared description of jointed rock masses by incorporating the mechanical characteristics of joints (stiffness, strength, and orientation) and layer thickness into the constitutive equations of the material. The finite element method based on the Cosserat continuum description incorporates the effects of discontinuities in the material constitutive equations. Combined finite element-joint methods and discrete element techniques, explicitly simulate the discontinuous surfaces.

This paper shows that the solution predicted by the FE-Cosserat method closely matches those predicted by methods that explicitly simulate joints. FE-Cosserat method however, is advantageous in that it uses a mesh which is totally independent of joint orientation and spacing. This aspect is of paramount importance in the solution of large scale problems and problems with complicated geometries due to presence of joints.

It is shown that the FE-Cosserat method is capable of capturing the dominant effects of discontinuous surfaces in deformation and strength. It is also capable of capturing scale effects resulting from material microstructures. However, due to the inherent assumptions of the constitutive equations of the Cosserat continuum, the FE-Cosserat solution is most appropriate in problems where microstructure follows a sequential pattern. Also, the method cannot capture mechanisms such as total detachment of rock blocks.

It is concluded that the Cosserat continuum and, in general, micropolar continuum theories can provide a mechanically based and practical solution to problems concerning materials with periodic microstructure. Research in the Cosserat description of material with microstructure therefore, may lead to reliable solutions to engineering scale problems that are deemed to be beyond current computational capabilities.

ACKNOWLEDGEMENTS

The authors gratefully acknowledge the financial support provided by the W.M. Keck Foundation for this research through the Digital Mine Project at the University of Toronto.

REFERENCES

Adhikary, D.P., Dyskin, A.V. 1997. A Cosserat continuum for layered materials. *Comput. and Geotech*. 20(1):15–45.

Adhikary, D.P., Dyskin A.V., 2007. Modelling of progressive and instantaneous failures of foliated rock slopes. *Rock Mech Rock Eng*. 40(4): 349–62.

Adhikary D.P., Mühlhaus H.B., Dyskin A.V., 1999. Modelling the large deformations in stratified media; the Cosserat continuum approach. *Mech. Cohes.-Frict. Mater*. 4(3):195–213.

Cosserat, E., Cosserat, F. 1909. *Theorie des corps deformables*. Hermann, Paris.

Eringen, A. 1999. *Microcontinuum field theories*. Springer, New York.

Eringen, A. 2002. *Nonlocal continuum field theories*. Springer, New York.

Forest, S., 2005. *Generalized Continua*. In Buschow, K., Cahn, R., Flemings, M., Ilschner, B., Kramer, E., and Mahajan, S., editors, *Encyclopedia of Materials: Science and Technology updates*, pages 1–7. Elsevier, Oxford.

Forest, S., *Mechanics of Cosserat media: An introduction*. Ecole des Mines de Paris / CNRS, Centre des Mat´eriaux / UMR 7633, BP 87, 91003 Evry, France. Internet.

Itasca Inc., 2004. 3DEC, *Three-dimensional Distinct Universal Code*, Version 4, Minneapolis, Minnesota, USA.

Mühlhaus, H.B. 1993. Continuum models for layered and blocky materials, *Comprehensive Rock Mechanics*. Pergamon Press. Oxford.

Mühlhaus, H.B. 1995. A relative gradient method for laminated materials. *Continuum Models for Materials with Microstructure*. Wiley.Toronto.

Mühlhaus, H.B., Vardoulakis, I. 1987. The thickness of shear bands in granular materials. *Geotechnique* (3): 271–83.

Riahi, A., 2008. 3D Finite Element Cosserat Continuum Simulation of layered Geomaterials. *Ph.D. Thesis*. University of Toronto.

Riahi, A., Curran, J.H. 2009. Full 3D finite element Cosserat formulation with application in layered structures. *Appl. Math. Model.,* 33:3450–64.

Riahi, A., Curran, J.H., Bidhendi, H. 2009. Buckling analysis of 3D layered structures using a Cosserat continuum approach. *Computers and Geotechnics*. 36: 1101–1112.

Riahi, A., Hammah, R.E., Curran, J.H., 2010. Limits of applicability of the finite element explicit joint model in the analysis of jointed rock problems, In *the Proceedings of the 44th ARMA Conference*, Salt Lake City, paper ID: 336

Rocscience Inc. 2005. *Phase²*, Version 6.0, Toronto, Canada.

Steinmann, P., 1994. A micropolar theory of finite deformation and finite rotation multiplicative elasto-plasticity. *Int. J. Solids Struct.*1(8): 1063–84.

Szilard, R., 2004. *Theories and applications of plate analysis: classical, numerical, and engineering methods*. Hoboken: John Wiley.

Truesdell, C., Toupin, R. 1960. *The classical field theories. Handbuch der Physik*, vol. 3. Berlin: Springer-Verlag.